Absorption edge, Urbach tail, and electron-phonon interactions in topological insulator Bi2Se3 and band insulator (Bi0.89In0.11)2Se3

Zhu, J.; Xia, Y.; Li, G.; Zhou, S.; Wimmer, S.; Springholz, G.; Pashkin, O.; Helm, M.; Schneider, H.;

Originally published:

April 2019

Applied Physics Letters 114(2019), 162105

DOI: https://doi.org/10.1063/1.5080790

Absorption edge, Urbach tail and electron-phonon interactions in topological insulator Bi_2Se_3 and band insulator $(Bi_{0.89}In_{0.11})_2Se_3$

Jiajun Zhu,[1,*] Yunyouyou Xia,[2] Gang Li,[2] Shengqiang Zhou,[1] S. Wimmer,[3] G. Springholz,[3] A. Pashkin,[1] M. Helm,[1,4] and H. Schneider[1,†]

[1]*Helmholtz-Zentrum Dresden Rossendorf, Institute of Ion Beam Physics and Materials Research, Bautzner Landstrasse 400, D-01328 Dresden, Germany*

[2]*School of Physical Science and Technology, ShanghaiTech University, Shanghai 201210, China*

[3]*Institut für Halbleiterphysik, Johannes Kepler Universität at Linz, 4040 Linz, Austria*

[4]*Institut für Angewandte Physik, TU Dresden, 01062 Dresden, Germany*

[*]j.j.zhu@foxmail.com

[†]h.schneider@hzdr.de

We employ infrared transmission spectroscopy to explore the temperature-dependent absorption edge and electron-phonon (*e-ph*) interaction in topological insulator Bi_2Se_3 and band insulator $(Bi_{0.89}In_{0.11})_2Se_3$ films. Upon heating from 5 K to 300 K, the absorption edge shifts from 262 to 249 meV for Bi_2Se_3 and from 367 to 343 meV for $(Bi_{0.89}In_{0.11})_2Se_3$. By analyzing the temperature dependence of the Urbach tail, the significant role of Raman-active phonon mode E_g^2 in *e-ph* interaction is identified, which agrees well with the *ab initio* calculation.

Topological insulators (TIs) are a class of quantum systems with an insulating bulk and a conducting surface. Their metallic surface states are formed by Dirac fermions with spin-momentum locking facilitated by strong spin-orbit coupling.[1,2] As an archetypical three-dimensional TI, Bi_2Se_3 has a large bulk gap of around 0.3 eV with the simplest surface state, opening up the possibility of many experiments. Indium doping in Bi_2Se_3 can effectively tune the spin-orbit coupling and drive the bulk topological phase transition. $(Bi_{1-x}In_x)_2Se_3$ shares the common rhombohedral D_{3d}^5 structure and a topological-to-trivial transition is observed in a range x from 0.03 to 0.07.[3,4] Despite intensive investigations of TIs, experimental studies for the temperature dependence of the optical gap in TIs are quite controversial. While Post *et al.* reported that TI $Bi_{2-x}Sb_x\ Te_{3-y}Se_y$ has an optical gap that shrinks with increasing temperature,[5] they found that the optical gap of $(Bi,\ Sb)_2Te_3$ does not show an apparent temperature dependence below room temperature.[6] There is a lack of comparison between the energy gap

and theoretical models, which could be used to show that temperature induced shifts are reasonable. Temperature dependences of the optical gap in TIs are seldom explained by any empirical model, such as Bose-Einstein model, in which the parameter is related to the known Debye temperature of the material.

At low temperatures, absorption spectrum of a pure semiconductor shows a definite edge, which can be used to determined optical gap, below which there is no absorption. In some materials, as the temperature is raised, a tail appears below the edge. This is the so-called Urbach tail, a well-known phenomenon in insulators with structural and thermal disorder, as these materials have localized states extended into the optical gap.[7] The temperature-dependent exponential parts of the absorption edge form an Urbach "bundle", which can be observed in both indirect and direct optical gap semiconductors.[8] The absorption process in the Urbach tail involves the simultaneous absorption of the photon together with any number of phonons.[9] Recently Martinez *et al* reported an almost exponential increase of the absorbance in TI Bi_2Se_3 reminiscent of the Urbach tail.[10] They focused on the evidence of the direct optical gap in Bi_2Se_3 without further analysis on the Urbach tail, which can provide important information about the *e-ph* interactions. Information on *e-ph* interactions can be obtained from absorption coefficient measurements near the absorption edge at different temperatures. Meanwhile, a systematic investigation of optical gap and Urbach tail in Bi_2Se_3 is lacking.

In this Letter, we address the temperature dependence of the absorption edge and the Urbach tail of TI Bi_2Se_3 by analyzing absorption data from infrared transmission measurements. The specific phonon mode participating in *e-ph* interactions of TI Bi_2Se_3 and $(Bi_{0.89}In_{0.11})_2Se_3$ is revealed, and it agrees well with Raman spectra and the first-principle calculations.

2-μm thick Bi_2Se_3 and $(Bi_{0.89}In_{0.11})_2Se_3$ films were grown on BaF_2 (111) substrates by molecular beam epitaxy under ultrahigh vacuum conditions of 5×10^{-10} mbar using Bi_2Se_3, In, and Se sources.[11] Transmission measurements were performed using a Bruker VERTEX 80 V Fourier transform infrared spectrometer in vacuum. The films were mounted into a continuous flow cryostat, controlled by a LakeShore 331 Temperature Controller. For Raman spectroscopy, a fiber-coupled iHR 550 micro-Raman setup (Horiba) with a 532 nm laser was used.

The phonon spectrum was calculated by applying supercell finite displacement method with PHONOPY[12] codes. To further evaluate the *e-ph* coupling strength, we determined the third-order interatomic force constants simplified from the anharmonic Hamiltonian in three phonon mode, as implemented in PHONO3PY[13] codes. In both processes, the force constants were calculated with Vienna *ab initio* simulation package (VASP) [14] based on the primitive cell optimized from the structure reported in Ref. [15] without including spin-orbit coupling. The exchange-correlation functional was considered in the generalized gradient approximation[16]. Employing the cut-off energy of 500 eV and the energy convergence criteria of 10^{-8} eV, we calculated the $2\times 2\times 2$ supercell using the **k**-point meshes of $2\times 2\times 2$. To visualize accurately the spectrum and linewidths, the phonon frequencies were finally sampled by $100\times 100\times 100$ **k**-point mesh.

Figs. 1(a) and 1(b) show the transmittance spectra of Bi_2Se_3 and $(Bi_{0.89}In_{0.11})_2Se_3$ films, respectively, normalized to the transmittance of the bare substrate. Due to the multiple reflections inside the film, the Fabry-Pérot interference can be observed in the transparent region. The absorption coefficient is obtained from the Beer-Lambert law and, thus, the reflection losses are not taken into account. This approximation should be plausible in the vicinity of and above the absorption edge due to the relatively large thickness of the measured films. The obtained absorption coefficients were subjected to a Fourier filtering in order to suppress the Fabry-Pérot fringes below the absorption edge. The high frequency cut-off indicates the direct transitions from the valence band to the conduction band. Since Bi_2Se_3 has a direct band gap at the Γ point,[17] in the vicinity of the absorption edge for $h\nu \geq E_G$, $(\alpha h\nu)^2$ is proportional to $(h\nu - E_G)$, where α is the absorption coefficient and E_G is the allowed direct optical gap. The plots of the quantity $(\alpha h\nu)^2$ as a function of photon energy for Bi_2Se_3 and $(Bi_{0.89}In_{0.11})_2Se_3$ films are shown in Figs. 1(c) and 1(d), respectively. The values of E_G can be obtained by extrapolating the linear portion of the curves to zero. The room temperature optical gap of Bi_2Se_3 films is 249 meV, which is smaller than the calculated value of 0.3 eV.[18] For single crystal Bi_2Se_3,[19] the variation of the optical gap from 0.25 to 0.35 eV depends on the n-type doping induced by Se vacancy content (Burstein-Moss shift).[20] Moreover, the optical gap of the thin film Bi_2Se_3 is thickness dependent. [21] The variation of the film thickness from 15 to 99 quintuple layers (1 quintuple layer ≈ 1 nm) results in the optical gap value from 0.19 to 0.25 eV, smaller than the value of single crystal due to in-gap impurity states.

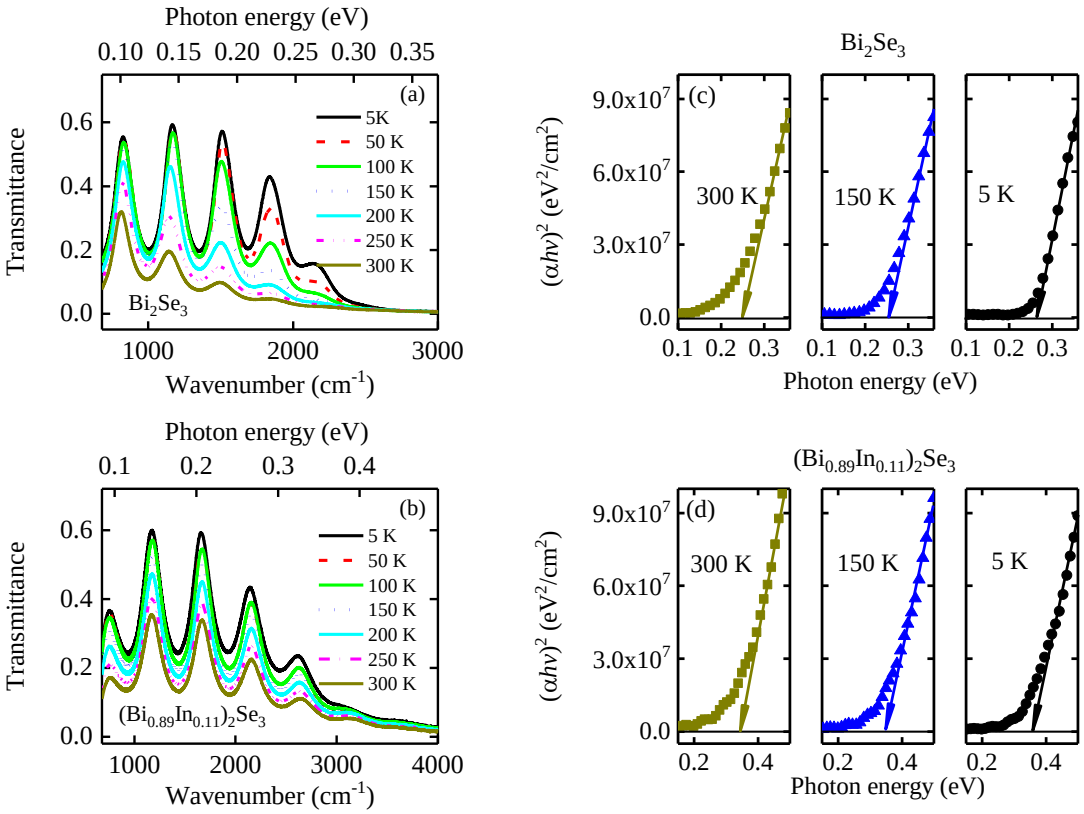

Figure 1. Transmittance spectra of 2-μm thick (a) Bi_2Se_3 and (b) $(Bi_{0.89}In_{0.11})_2Se_3$ films at temperatures of 5, 50, 100, 150, 200, 250, and 300 K. The variation in $(\alpha hv)^2$ as a function of photon energy for (c) Bi_2Se_3 and (d) $(Bi_{0.89}In_{0.11})_2Se_3$ films is used to determine the optical gap energy E_G.

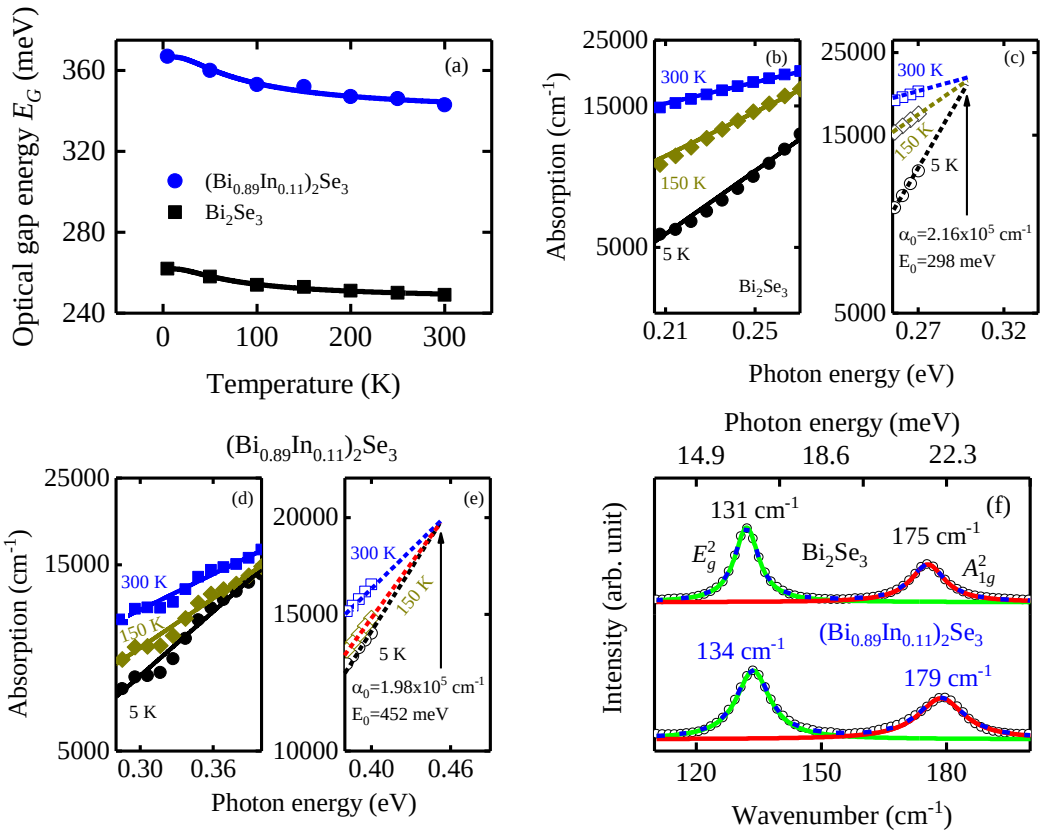

Figure 2. (a) Temperature dependence of the optical gap energy E_G for Bi_2Se_3 and $(Bi_{0.89}In_{0.11})_2Se_3$ films. The fitting results using Eq.(1) are plotted as solid lines. (b)-(e) Absorption coefficient α of Bi_2Se_3 and $(Bi_{0.89}In_{0.11})_2Se_3$ films below the optical gap. Solid lines in (b) and (d) represent the fitting results by the Urbach model. Dashed lines in (c) and (e) are guides to the eye. (f) Raman spectra of Bi_2Se_3 and $(Bi_{0.89}In_{0.11})_2Se_3$ films. Lorentz model is used to fit the peaks.

Fig. 2(a) shows that the optical gap of $(Bi_{0.89}In_{0.11})_2Se_3$ films is 343 meV at room temperature, larger than the value 249 meV of Bi_2Se_3 films. This is due to a topological phase transition occurring by closing and reopening of the bandgap at x around 0.06.[3] The optical gap of Bi_2Se_3 or $(Bi_{0.89}In_{0.11})_2Se_3$ films presents a blueshift trend with decreasing temperature. Thermal expansion and *e-ph* coupling contribute to the temperature dependence of band structures in Bi_2Se_3 family of compounds. First-principle calculations[22] reveal that the effect of thermal expansion is more important in TI Bi_2Se_3 due to the heavy elements as compared to materials made of light atoms, such as silicon and germanium.[23]

The temperature dependence of the optical gap can be described by a Bose-Einstein expression[24]

$E_G(T)= E_G$ (T=0 K)-$2a_B$/[exp(Θ_B/T)-1] (Eq.(1)), where T is the temperature, a_B is the phonon-induced lifetime broadening of the electronic states at T=0, and Θ_B is the characteristic phonon temperature. The fitting results are listed in Table 1. The optical gap E_G of Bi_2Se_3 toward 0 K is 262±0.5 meV, smaller than that of $(Bi_{0.89}In_{0.11})_2Se_3$ with the value of 367±21.5 meV. The broadening is produced by the electron-phonon interaction and their temperature dependence. This effect can be described by a complex self-energy of the electronic states.[25] The real part of this self-energy is responsible for a shift of the bands with temperature, while the imaginary part is related to the broadening of the electronic states. In our case, a_B is 2.9 meV for Bi_2Se_3, smaller than 5.3 meV for $(Bi_{0.89}In_{0.11})_2Se_3$ due to increased disorder in $(Bi_{0.89}In_{0.11})_2Se_3$. The average phonon temperature Θ_B of Bi_2Se_3 is 73±9 K, and the corresponding Debye temperature Θ_D can be calculated by $\Theta_D= 8\Theta_B/3$.[26] Debye temperature Θ_D is 195±23.5 K for Bi_2Se_3 and 211±41.6 K for $(Bi_{0.89}In_{0.11})_2Se_3$, which agrees well with the reported value of 185 K for bulk Bi_2Se_3.[27]

Table 1

The parameter values of Eq.(1) obtained from the fit of the experiments and Debye temperature $\Theta_D= 8\Theta_B/3$.

Sample	E_G (T=0 K) meV	a_B (meV)	Θ_B (K)	Θ_D (K)
Bi_2Se_3	261.9±0.5	2.9±0.1	73.3±8.8	195±23.5
$(Bi_{0.89}In_{0.11})_2Se_3$	366.7±1.5	5.3±0.4	79.8±15.6	211±41.6

Below the optical gap, the absorption coefficient α follows an exponential energy dependence. The absorption in this regime can be fitted by the Urbach model:

$$\alpha(E) = \alpha_0 \exp[\sigma(T)\frac{E-E_0}{k_B T}], \qquad (2)$$

where α_0 and E_0 are the coordinates of the convergence point of the Urbach "bundle", k_B is Boltzmann constant, σ is the steepness parameter, T is the temperature. The Urbach energy is defined as $E_U=k_BT/\sigma(T)$, which is related to the width of the optical band tail due to localized states in the material optical gap that are associated with the disordered or low-quality crystalline materials. Figs. 2(b)-(e) show the absorption coefficients α of Bi_2Se_3 and $(Bi_{0.89}In_{0.11})_2Se_3$ films. The exponential increase of the absorption coefficient near the absorption edge is due to the transitions between the tails of density of states in the valence band and the conduction band. Figs. 2(c) and 2(d) show that the linear parts of absorption coefficient converge to one point. The coordinates of this convergence point α_0 is 2.16×10^5

cm^{-1} and E_0 is 298 meV for Bi_2Se_3, while α_0 is 1.98×10^5 cm^{-1} and E_0 is 452 meV for $(Bi_{0.89}In_{0.11})_2Se_3$. Raman spectra in Fig. 2(f) will be discussed later.

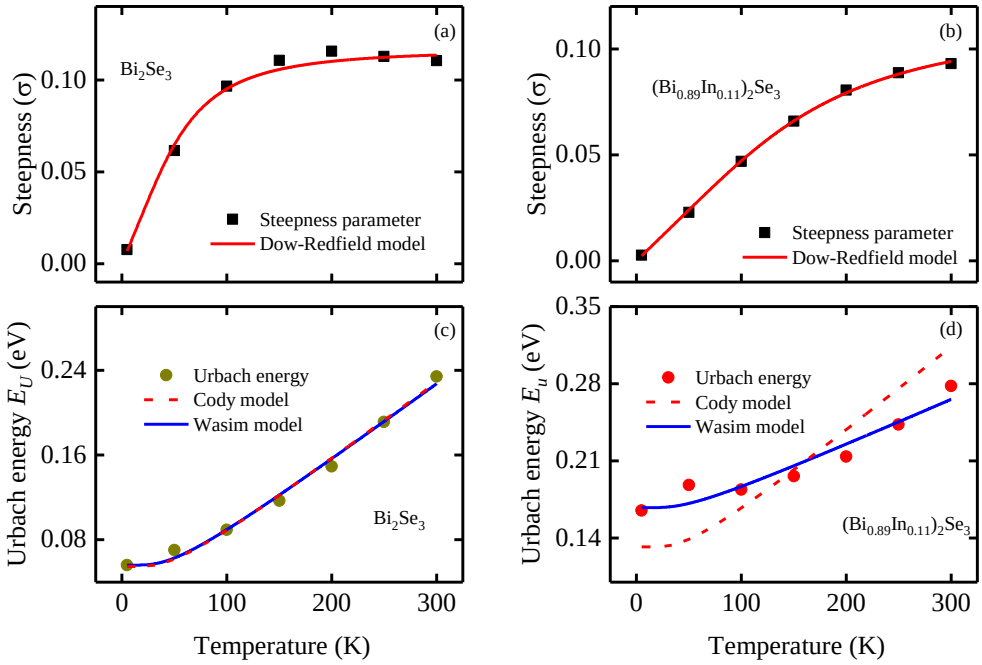

Figure 3. Steepness parameter of (a) Bi_2Se_3 and (b) $(Bi_{0.89}In_{0.11})_2Se_3$ films. Urbach energy E_U of (c) Bi_2Se_3 and (d) $(Bi_{0.89}In_{0.11})_2Se_3$ films. Symbols: Experimental data. Solid/dashed lines: Fits using the models as described in the text.

According to the phonon theory, Dow and Redfield[28] give the relationship between the steepness parameter σ of the Urbach tail, temperature and phonon energy as

$$\sigma(T) = \sigma_0 \frac{2k_BT}{\hbar\omega}\tanh(\frac{\hbar\omega}{2k_BT}), \qquad (3)$$

where σ_0 is a temperature independent constant describing the optical excitation in the material and $\hbar\omega$ represents the phonon energy which coincides with the energy of the phonons participating in the formation of the long-wave side of the fundamental absorption edge. The interaction of electrons and/or excitons with phonons influences the Urbach tail. The temperature dependent steepness parameter σ_0 of Bi_2Se_3 and $(Bi_{0.89}In_{0.11})_2Se_3$ films is shown in Figs. 3(a) and 3(b), respectively. From the fitting values shown in Fig. 3, the phonon energy $\hbar\omega$ for Bi_2Se_3 is 14.5 meV, which is very close to the E_g^2 mode at 17.4 meV from calculations or at 16.6 meV from Raman measurement. For $(Bi_{0.89}In_{0.11})_2Se_3$, the resulting phonon energy $\hbar\omega$ is 40.3 meV, which is much larger than any actual phonon energy. The

possibility of the electron interacting with multiple phonons is much lower than that with a single phonon, therefore, we need to consider the disorder of the sample, which significantly influences the phonon energy determined from the Urbach tail.

Table 2: The parameter values of Eq.(3).

Sample	σ_0	$h\omega$ (meV)
Bi_2Se_3	0.117±0.004	14.47±0.002
$(Bi_{0.89}In_{0.11})_2Se_3$	0.112±0.002	40.34±0.001

Table 3: The parameter values of Eq.(4).

Sample	P	N
Bi_2Se_3	0.076±0.042	1
$(Bi_{0.89}In_{0.11})_2Se_3$	1.471±0.237	1
	2.325±0.135	0.574±0.072

Fig.3(c) shows that the Urbach energy is 56 meV for Bi_2Se_3 at T=5 K, which is quite reasonable and much smaller than its optical gap of 262 meV at T=5 K. Figs. 3(c) and 3(d) show that the Urbach energy increases very slowly below 150 K because the number of the thermally induced phonon is very low and the weak temperature dependence is related to the structural disorder. By comparison, the Urbach energy increases very rapidly above 200K, indicating a higher phonon occupation with increase of the temperature. It is not surprising to find that the Urbach energy of indium doped Bi_2Se_3 is larger than that of pure Bi_2Se_3, as the Urbach energy is related to the crystalline lattice disorder caused by structural peculiarities and external factors. For pure Bi_2Se_3, the Urbach energy is related to thermal broadening and structural disorder. The thermal broadening is mainly caused by the lattice thermal vibrations. The structural disordering of Bi_2Se_3 is caused by intrinsic defects, e.g., Se vacancies or interstitials, while the external factor, such as indium doping effects, plays an important role in $(Bi_{0.89}In_{0.11})_2Se_3$. To consider the disorder, we fit the Urbach energy by Cody model[29]

$$E_U(T) = \frac{3k_B\Theta_D}{4\sigma_0}\left[\frac{1+P}{2} + \frac{\mathrm{N}}{\exp(3\Theta_D/4T)-1}\right], \quad (4)$$

where P is the structural disorder associated with stoichiometry of the films, and N equals to one. Fig. 3(c) shows that the Urbach energy of Bi_2Se_3 can be fitted quite well by Cody model,

which reflects very few defects and disorder in Bi_2Se_3. Due to increased lattice and alloy disorder, the Urbach energy of $(Bi_{0.89}In_{0.11})_2Se_3$ can not be fitted well by Cody model, as shown in Fig. 3(d). In this case, we consider a revised model proposed by Wasim *et al.*[30] with a free parameter N, which is the fraction of the total phonon modes excited at a given temperature which can interact with excitons electrons due to structural disorder. In Wasim model, for Bi_2Se_3, P = 0.114 which is smaller than P = 2.325 of $(Bi_{0.89}In_{0.11})_2Se_3$. N is 0.998 for Bi_2Se_3, quite close to 1 as for an ideal ordered system, while for the $(Bi_{0.89}In_{0.11})_2Se_3$, N is 0.574, which is much smaller. Both values of P and N are quite reasonable, as indium doped Bi_2Se_3 is expected to have a larger structural disorder than pure Bi_2Se_3 due to the presence of a large number of unintended impurities and vacancies as a result of doping as well as due to alloy disorder. The parameters P and N of $(Bi_{0.89}In_{0.11})_2Se_3$ deviate a lot from the ideal ordered system. Because the idealized Urbach tail model does not account for the sorts of defects, the phonon energy $\hbar\omega$ (40.3 meV) obtained in this way is much larger than any actual phonon energy.

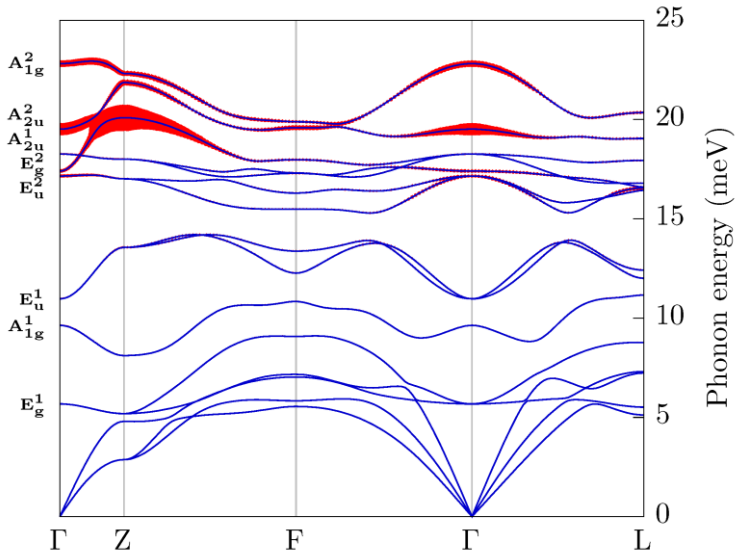

Figure 4. Phonon spectrum for Bi_2Se_3 with the radii of red circles denoting the magnitude of phonon linewidths.

Fig. 2(d) shows Raman spectra of Bi_2Se_3 and $(Bi_{0.89}In_{0.11})_2Se_3$ films. For Bi_2Se_3, the peaks at 131 and 175 cm^{-1} are E_g^2 and A_{1g}^2 modes, respectively. The frequencies of these modes in $(Bi_{0.89}In_{0.11})_2Se_3$ shift to 134 and 179 cm^{-1} due to the lighter indium mass compared to bismuth. For Bi_2Se_3, the phonon linewidth (full width at half maximum, FWHM) of E_g^2 is 7.1 cm^{-1} and that of A_{1g}^2 is 10 cm^{-1}. For $(Bi_{0.89}In_{0.11})_2Se_3$, the phonon linewidth of E_g^2 is 9.8 cm^{-1} and that of A_{1g}^2 is 13.5 cm^{-1}. Both peaks FWHM broaden due to disorder. The calculated

phonon frequencies at the Γ point in unit of meV are 5.68, 9.63, 10.97, 17.16, 17.41, 18.26, 19.52, and 22.82, corresponding to the modes E_g^1, A_{1g}^1, E_u^1, E_u^2, E_g^2, A_{2u}^1, A_{2u}^2, and A_{1g}^2, respectively. The calculated phonon spectrum in Fig. 4 shows that the Raman-active mode E_g^2 at Γ point around 17.41 meV has the largest magnitude of phonon linewidth. Since phonon linewidth, the twice of the imaginary part of the phonon self-energy, is a measure of the amount of *e-ph* coupling contributed by each phonon mode, we here identify E_g^2 to be the most active phonon mode participating in *e-ph* interaction.

Urbach tails are observed in the absorption spectra of Bi_2Se_3 and $(Bi_{0.89}In_{0.11})_2Se_3$ films. The phonon energy $h\omega$ associated with the Urbach tail is 14.47 meV for Bi_2Se_3. Calculations show that the Raman-active mode E_g^2 with the largest magnitude of phonon linewidths is the most probable phonon mode participating in *e-ph* interaction. E_g^2 is found to be at 17.41 meV from calculations and 16.6 meV from Raman measurements, which agrees well with the analysis of the Urbach tail.

We would like to thank Dr. Matthias Krause (HZDR) for Raman measurements. Support by the Austrian Science Funds FWF, Projects P28185-N27 and P29630-N27 is also acknowledged.

[1] M. Z. Hasan and C. L. Kane, Rev. Mod. Phys. 82, 3045 (2010).
[2] X. L. Qi and S. C. Zhang, Rev. Mod. Phys.83, 1057 (2011).
[3] L. Wu, M. Brahlek, R. V. Aguilar, A. V. Stier, C. M. Morris, Z. Lubashevskz, L. S. Bilbro, N. Bansal, S. Oh, and N. P. Armitage, Nat. Phys. 9, 410 (2013).
[4] M. Salehi, H. Shapourian, N. Koirala, M. J. Brahlek, J. Moon, and S. Oh, Nano Lett. 16, 5528 (2016).
[5] K. W. Post, Y. S. Lee, B. C. Chapler, A. A. Schafgans, Mario Novak, A. A. Taskin, Kouji Segawa, M. D. Goldflam, H. T. Stinson, Yoichi Ando, and D. N. Basov, Phys. Rev. B 91, 165202 (2015).
[6] K. W. Post, B. C. Chapler, M. K. Liu, J. S. Wu, H. T. Stinson, M. D. Goldflam, A. R. Richardella, J. S. Lee, A. A. Reijnders, K. S. Burch, M. M. Fogler, N. Samarth, and D. N. Basov, Phys. Rev. Lett. 115, 116804 (2015).
[7] F. Urbach, Phys. Rev. 92, 1324 (1953).
[8] S. John, C. Soukoulis, M. H. Cohen, and E. N. Economou, Phys. Rev. Lett. 57, 1777 (1986).
[9] D. Dunn, Phys. Rev. 174, 855 (1968).
[10] G. Martinez, B. A. Piot, M. Hakl, M. Potemski, Y. S. Hor, A. Materna, S. G. Strzelecka, A. Hruban, O. Caha, J. Novák, A. Dubroka, Č. Drašar, and M. Orlita, Sci. Rep. 7, 6891 (2017).
[11] J. Zhu, F. Liu, S. Zhou, C. Franke, S. Wimmer, V. V. Volobuev, G. Springholz, A. Pashkin, H. Schneider, and M. Helm, Appl. Phys. Lett. 109, 202103 (2016).
[12] A. Togo and I. Tanaka, Scr. Mater. 108, 1-5 (2015).
[13] A. Togo, L. Chaput, and I. Tanaka, Phys. Rev. B 91, 094306 (2015).
[14] G. Kresse and J. Furthmüller, Phys. Rev. B 54, 11169 (1996).
[15] S. Nakajima, Journal of Physics and Chemistry of Solids 24, 479 (1963).

[16] J. P. Perdew, K. Burke, and M. Ernzerhof, Phys. Rev. Lett. 77, 3865 (1996).
[17] I. A. Nechaev, R. C. Hatch, M. Bianchi, D. Guan, C. Friedrich, I. Aguilera, J. L. Mi, B. B. Iversen, S. Blügel, Ph. Hofmann, and E. V. Chulkov, Phys. Rev. B 87, 121111(R) (2013).
[18] Haijun Zhang, Chao-Xing Liu, Xiao-Liang Qi, Xi Dai, Zhong Fang, and Shou-Cheng Zhang, Nat. Phys. 5, 438 (2009).
[19] P. Di Pietro, F. M. Vitucci, D. Nicoletti, L. Baldassarre, P. Calvani, R. Cava, Y. S. Hor, U. Schade, and S. Lupi, Phy. Rev. B 86, 045439 (2012).
[20] A. Dubroka, O. Caha, M. Hronček, P. Friš, M. Orlita, V. Holý, H. Steiner, G. Bauer, G. Springholz, and J. Humlíček, Phy. Rev. B 96, 235202 (2017).
[21] K. W. Post, B. C. Chapler, L. He, X. Kou, K. L. Wang, and D. N. Basov, Phys. Rev. B 88, 075121 (2013).
[22] B. Monserrat and D. Vanderbilt, Phys. Rev. Lett. 117, 226801 (2016).
[23] D. F. Gibbons, Phys. Rev. 112, 136 (1958).
[24] J. J. Zhu, W. W. Li, G. S. Xu, K. Jiang, Z. G. Hu, and J. H. Chu, Acta Mater 59, 6684 (2011).
[25] P. Lautenschlager, P. B. Allen, and M. Cardona, Phys. Rev. B 33, 5501 (1986).
[26] R. C. Rai, J. Appl. Phys. 113, 153508 (2013).
[27] X. X. Yang, Z. F. Zhou, Y. Wang, R. Jiang, W. T. Zheng, and C. Q. Sun, J. Appl. Phys. 112, 083508 (2012).
[28] J. D. Dow and D. Redfield, Phys. Rev. B 5, 594 (1972).
[29] G. D. Cody, T. Tiedje, B. Abeles, B. Brooks, and Y. Goldstein, Phys. Rev. Lett. 47, 1480 (1981).
[30] S. M. Wasim, G. Marin, C. Rincon, and G. S. Perez, J. Appl. Phys.84, 5823 (1998).